

Measurement of isotope shifts, fine and hyperfine structure splittings of the lithium D lines

J. Walls, R. Ashby, J.J. Clarke, B. Lu, and W.A. van Wijngaarden^a

Physics Department, Petrie Bldg., York University, 4700 Keele St. Toronto, Ontario M3J 1P3, Canada

Received 8 April 2002 / Received in final form 26 June 2002

Published online 21 January 2003 – © EDP Sciences, Società Italiana di Fisica, Springer-Verlag 2003

Abstract. The lithium D lines were studied using a diode laser that was frequency modulated by an electro-optic modulator, to excite an atomic beam. The transmission of part of the laser beam through an etalon was monitored to correct for the nonlinearity of the laser scan. The results for the $^{6,7}\text{Li}$ $2S_{1/2}$ and $2P_{1/2}$ hyperfine splittings agree very well with the best existing data while those for the D1 isotope shift and $^{6,7}\text{Li}$ fine structure splittings disagree significantly from data obtained by a previous laser atomic beam experiment. Our result for the D1 isotope shift is very close to the latest value computed using Hylleraas variational theory.

PACS. 32.10.Fn Fine and hyperfine structure – 32.30.Jc Visible and ultraviolet spectra

Significant advances in the last decade have been made in the theoretical modeling of few electron atoms and of neutral lithium in particular [1–5]. The models are sensitive to the nuclear size. Hence, high precision measurements of isotope shifts yield information similar but in some cases more accurate than that obtained in nuclear scattering experiments [6]. Experimental progress is therefore making lithium an interesting testing ground for theory and may also provide opportunities to determine improved values of fundamental constants such as the fine structure constant [7].

The various energy levels contributing to the structure of the lithium D lines are shown in Figure 1. A variety of techniques have been used to measure the $^{6,7}\text{Li}$ isotope shift as well as the fine and hyperfine structure splittings of the Li D lines including level crossing [8,9], optical double resonance [10–12], Fourier transform [13] and frequency modulation spectroscopy [14]. The most popular experimental technique is to excite an atomic beam using a laser beam that is directed perpendicularly to the atom's velocity to minimize Doppler broadening [15–19]. Fluorescence is detected as the laser frequency is scanned across the transition. The change in laser frequency is monitored by passing part of the laser beam through an etalon producing a series of transmission peaks separated by the cavity's free spectral range. The accurate determination of the free spectral range or the etalon length can be problematic and some measurements have needed to be redone [17]. This work, unlike other experiments, simultaneously determined the $^{6,7}\text{Li}$ isotope shift of the D lines as well as the hyperfine (HFS) and fine structure (FS) splittings of

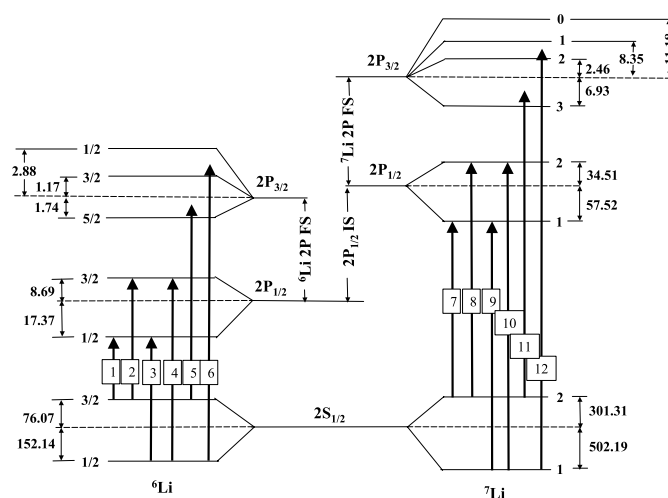


Fig. 1. Relevant lithium energy levels. The frequency intervals listed are taken using data found in the literature [12, 17–19]. The vertical energy axis is not drawn to scale. The position of the various hyperfine levels is indicated relative to the center of gravity energy of a state $E_{CG} = \sum_F (2F + 1) E_F / \sum_F (2F + 1)$ where E_F is the energy of hyperfine level F . The transitions indicated were excited in this experiment as shown in Figures 3 and 4.

the $2S_{1/2}$ and $2P_{1/2}$ states, permitting important consistency checks. Moreover, the results do not rely on any calibration of an etalon's free spectral range by a separate experimental apparatus.

An overview of the apparatus is shown in Figure 2 and is described in detail elsewhere [20]. An atomic beam having a divergence of less than 0.5 milliradians was generated

^a e-mail: wvw@yorku.ca

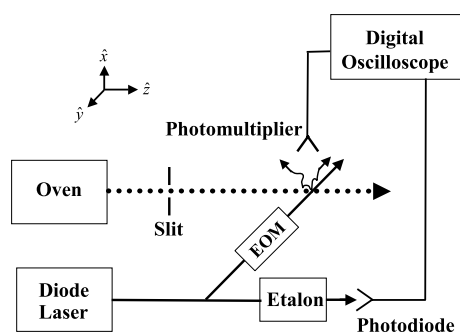


Fig. 2. Apparatus. See text for description.

by heating a sample of lithium metal to several hundred degrees centigrade. The oven was enclosed in a vacuum chamber pumped using a diffusion pump and a liquid nitrogen trap to a pressure of about 1×10^{-7} torr. The lithium atoms were excited using a diode laser (Tuioptics Model DL100/670) that produced a laser beam having a power of 12 mW at 670 nm. The laser was frequency modulated using either a 6.8 or 9.2 GHz electro-optic modulator (ν -focus 4851). The modulation frequency was specified by a frequency synthesizer (Agilent E8241A) to one part in 10^7 and chosen such that the various fluorescent peaks did not overlap. The laser beam was linearly polarized along the \hat{z} -direction parallel to the atomic beam.

The laser frequency could be scanned up to 15 GHz by adjusting a grating. The linearity of the laser scan was monitored by passing part of the laser beam through a confocal etalon having a free spectral range of nearly 300 MHz. The etalon was constructed using an invar rod to minimize temperature variation effects. A photodiode (PD) monitored the laser beam transmitted through the etalon.

Fluorescence emitted in the \hat{x} -direction was detected by a photomultiplier (PMT – Hamamatsu R928). The photomultiplier and photodiode signals were stored in a digital oscilloscope (Tektronix TDS3052). A single laser scan generated a data file having 10,000 points. A total of 218 separate laser scans were taken using a sample of pure ^6Li yielding spectra as shown in Figure 3. An additional 244 scans as shown in Figure 4 were taken using a natural sample of lithium. Scans like that shown in Figure 4 used the 6.8 GHz modulator instead of the 9.2 GHz modulator to avoid overlap of the fluorescence peaks.

Data was analyzed using the SOLVER feature of Microsoft Excel (version 9.0) and a Fortran computer program. The fluorescence peak positions were found by fitting a sum of Lorentzian functions to the peaks in the spectrum. Similarly, the location of the Fabry-Perot transmission peaks were found. The position of a fluorescence peak relative to the nearest Fabry-Perot peak was determined using a 5th order polynomial to interpolate between the 6 nearest Fabry-Perot peak centers. This was done to account for the nonlinearity of the laser frequency scan. The free spectral range of the etalon was determined using the electro-optic modulation frequency intervals as shown in Figures 3 and 4.

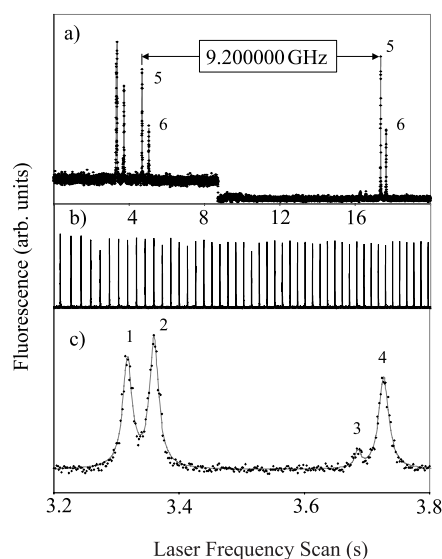


Fig. 3. Sample ^6Li Laser Scan. Figure (a) shows the fluorescence (black dots) taken during a laser frequency scan along with the fitted spectrum. Each transition is excited twice due to electro-optically modulating the laser frequency at 9.2 GHz. A neutral density filter was inserted midway during the scan to avoid saturating the photomultiplier by the D2 line. Figure (b) shows the transmission of part of the laser beam through an etalon. The first two peaks shown in (a) are the ^6Li D1 lines and are actually 4 peaks as shown in (c).

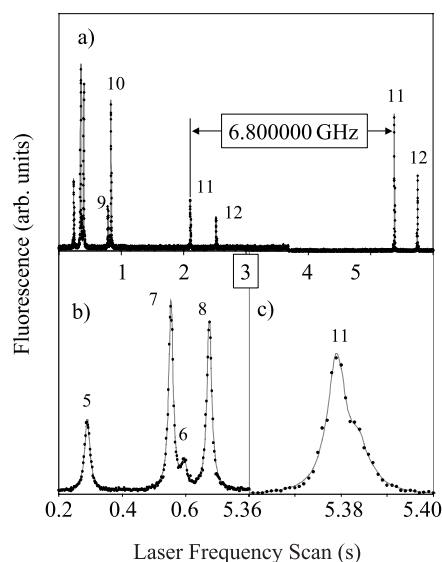


Fig. 4. Sample ^7Li Laser Scan. Figure (a) shows the fluorescence (black dots) taken during a laser scan using a 6.8 GHz electro-optic modulator along with the fitted spectrum. A neutral density filter was inserted midway during the scan to avoid saturating the photomultiplier by the D2 transition. The first few peaks not labelled in (a) are highlighted in (b). Figure (c) shows the D2 peak resulting from the excitation of the ^7Li $2S_{1/2}$ ($F = 2$) hyperfine level to the $2P_{3/2}$ state. The asymmetric shape is due to the partial resolution of the hyperfine structure of the $2P_{3/2}$ state as is described in the text.

A stringent test of the experimental method was to compare our result for the ${}^6,{}^7\text{Li}$ ground state hyperfine splittings with those obtained using an atomic beam magnetic resonance experiment [21]. The ${}^6\text{Li}$ $2S_{1/2}$ hyperfine interval was found by measuring the frequency separating peaks 2 and 4 while the ${}^6\text{Li}$ $2P_{1/2}$ hyperfine interval was determined using peaks 1 and 2. Peak 3 was not used as it is substantially smaller. For ${}^7\text{Li}$, the ground state hyperfine splitting found using the separation between peaks 7 and 9 (803.49 ± 0.11 MHz) agreed with that obtained using peaks 8 and 10 (803.57 ± 0.10 MHz). Similarly, the ${}^7\text{Li}$ $2P_{1/2}$ hyperfine interval found from the separation of peaks 7 and 8 (91.94 ± 0.08 MHz) agreed with that found using peaks 9 and 10 (92.10 ± 0.07 MHz). Table 1 shows excellent agreement of our results with the published data. The listed uncertainties are one standard deviation of the data from the average value. The results for the ${}^6,{}^7\text{Li}$ $2P_{1/2}$ magnetic dipole hyperfine constant a have an uncertainty comparable to the best published values. Our value for $a({}^7\text{Li } 2P_{1/2})$ is 96 kHz higher than that obtained in an optical double resonance experiment [12] where the uncertainty of each measurement is 25 kHz. It is interesting that recent predictions found using multiconfiguration Hartree-Fock theory lie between the two most precise experimental results.

A complication in determining the ${}^6\text{Li}$ fine structure splitting is that the hyperfine splitting of the ${}^6\text{Li}$ $2P_{3/2}$ state [10,11] is smaller than the 5.8 MHz FWHM natural linewidth of the $2P-2S_{1/2}$ transition [22]. In addition, the laser does not excite the hyperfine levels equally. For ${}^6\text{Li}$, the $2S_{1/2}$ ($F = 1/2$) hyperfine level can only be laser excited to the $2P_{3/2}$ ($F = 1/2, 3/2$) hyperfine levels. Moreover, these two hyperfine levels contribute differently to the observed fluorescence due to their respective transition Clebsch-Gordan coefficients [23]. A computer program was written to model the effect of optical pumping resulting from repeated laser excitation and fluorescence decay as an atom passed through the laser beam [24]. It was found that the fluorescence signal observed by exciting the $2S_{1/2}$ ($F = 1/2$) level to the $2P_{3/2}$ state is +1.90 MHz above the $2P_{3/2}$ center of gravity indicated in Figure 1. Similarly, the fluorescence signal observed by exciting the $2S_{1/2}$ ($F = 3/2$) level to the $2P_{3/2}$ state is 1.27 MHz below the $2P_{3/2}$ center of gravity. The results listed in Table 1 for the ${}^6\text{Li}$ fine structure have been corrected for this effect. A test of these corrections was made by determining the $2S_{1/2}$ hyperfine splitting using the D2 line. The measured value for the separation between peaks 5 and 6 was 231.327 ± 0.050 MHz. Taking into account the two corrections given above yields a ground state hyperfine splitting of 228.157 ± 0.050 MHz, in excellent agreement with the accepted value.

For the ${}^7\text{Li}$ D2 line, the laser excitation partially resolves the $2P_{3/2}$ ($F = 1, 2, 3$) hyperfine splitting although the $F = 3$ hyperfine level predominates the fluorescence signal as shown in Figure 4c. Peak 11 was fitted using three Lorentzians where the relative center frequencies were constrained to equal the intervals separating the $F = 1$ & 2 and $F = 2$ & 3 hyperfine levels of the $2P_{3/2}$ state [12].

Table 1. Comparison of Results to Published Data. FM = Frequency Modulation, FT = Fourier Transform, LAB = Laser Atomic Beam, LC = Level Crossing, ODR = Optical Double Resonance, FCPC = Full Core plus Correlation, HV = Hylleraas Variational Calculation, MCHF = Multiconfigurational Hartree-Fock, MCHFc = MCHF plus relativistic corrections.

Quantity	Result (MHz)	Reference
${}^6\text{Li } 2S_{1/2}$ HFS	228.205259	ABMR [21]
	228.164 ± 0.064	this work
${}^6\text{Li } a(2P_{1/2})$	17.48 ± 0.15	ODR [10]
	17.375 ± 0.018	ODR [12]
	17.8 ± 0.3	LC [9]
	16.8 ± 0.7	LAB [17]
${}^6\text{Li } 2P$ FS	17.386 ± 0.031	this work
	$10\ 052.76 \pm 0.22$	LC [8]
	$10\ 050.2 \pm 1.5$	LAB [17]
	$10\ 051.62 \pm 0.20$	LAB [19]
	$10\ 053.044 \pm 0.091$	this work
${}^7\text{Li } 2S_{1/2}$ HFS	$10\ 050.846 \pm 0.012$	HV [1]
	803.5040866	ABMR [21]
${}^7\text{Li } a(2P_{1/2})$	803.534 ± 0.077	this work
	46.17 ± 0.35	ODR [10]
	45.914 ± 0.025	ODR [11]
	46.05 ± 0.30	LAB [17]
	46.010 ± 0.025	this work
${}^7\text{Li } 2P$ FS	45.793	FCPC [2]
	45.984 ± 0.007	MCHF [3]
	45.945	MCHFc [5]
	$10\ 053.24 \pm 0.22$	LC [8]
	$10\ 053.184 \pm 0.058$	ODR [11]
	$10\ 056.6 \pm 1.5$	LAB [17]
	$10\ 053.2 \pm 1.4$	LAB [18]
	$10\ 053.4 \pm 0.2$	LAB [19]
D1 isotope shift	$10\ 052.37 \pm 0.11$	this work
	$10\ 051.214 \pm 0.012$	HV [25]
	10 532 ± 5	LAB [15]
	$10\ 534.3 \pm 0.3$	LAB [17]
	$10\ 532.9 \pm 0.6$	FM [14]
	$10\ 526 \pm 15$	FTS [13]
	$10\ 533.13 \pm 0.15$	LAB [19]
	$10\ 534.26 \pm 0.13$	this work
	10 528.7	MCHF [5]
	$10\ 534.31 \pm 0.68$	HV [4]
$10\ 534.12 \pm 0.07$	HV [25]	

The ${}^7\text{Li}$ fine structure was determined by measuring the separation of peaks 10 and 11. Peak 12 was not analyzed because the intervals separating the $2P_{3/2}$ ($F = 0, 1, 2$) levels are smaller than is the case for peak 11 making it more difficult to model precisely. The D1 isotope shift was determined by measuring the separation of peaks 5 and 7 shown in Figure 4 and using the ${}^6\text{Li}$ fine structure splitting as determined in Figure 3.

Our result for the ${}^6\text{Li}$ fine structure splitting has the smallest uncertainty of any experimental determination. It is the only laser atomic beam result that agrees with the result of a level crossing experiment. Our ${}^7\text{Li}$ fine structure splitting is slightly smaller than that found previously. This may be due to our partial resolution of the $2P_{3/2}$ hyperfine splitting described in the preceding paragraph as it is not clear how some of the other experiments accounted for this effect. The theoretical estimates for the ${}^6,7\text{Li}$ fine structure splittings are 1–2 MHz below the experimental data [1]. This is not surprising as only terms in the Hamiltonian of order α^3 where α is the fine structure constant, were considered. For the case of helium, the terms of order α^4 contribute several MHz to the fine structure splitting.

The result for the D1 isotope shift is over 1 MHz higher than the other most accurate laser atomic beam result. However, our value agrees very well with the result of the latest Hylleraas variational calculation [25] which refines an earlier estimate [4] that took into account the finite nuclear size as well as QED terms up to order $(\mu/M)\alpha^3$ where μ is the electronic reduced mass and M is the nuclear mass. All of the experimental values are significantly higher than a result found using multiconfiguration Hartree-Fock theory.

In conclusion, this experiment has simultaneously obtained data for the ${}^6,7\text{Li}$ isotope shift, fine structure and hyperfine splittings of the $2S_{1/2}$ and $2P_{1/2}$ states. The results are consistent with very accurate measurements of the ground state hyperfine splitting. The values obtained for the fine structure and D1 isotope shift disagree with previous laser atomic beam measurements but are in better agreement with the latest theoretical predictions. A key advantage of the present experiment is that it does not rely on the determination of an etalon's free spectral range by a secondary experiment. Each scan is separately calibrated using the electro-optic modulation frequency. Hence, the experimental method has wide applicability for precision laser spectroscopic measurements.

The authors would like to thank the Natural Science and Engineering Research Council of Canada and the Canadian Institute for Photonic Innovations for financial support. J. Walls

and J. Clarke are the recipients of Ontario Graduate and JDS scholarships respectively. We thank A. Madej for his donation of an invar rod and G.W.F. Drake for insightful comments.

References

1. Z.C. Yan, G.W.F. Drake, Phys. Rev. Lett. **79**, 1646 (1997)
2. X.X. Guan, Z.W. Wang, Eur. Phys. J. D **2**, 21 (1998)
3. N. Yamanaka, J. Phys. Soc. Jap. **68**, 2561 (1999)
4. Z.C. Yan, G.W.F. Drake, Phys. Rev. A **61**, 22504-1 (2000)
5. M. Goedfroid, C.F. Fischer, P. Jonsson, J. Phys. B **34**, 1079 (2001)
6. E. Riis *et al.*, Phys. Rev. A **49**, 207 (1994)
7. W. Frieze, E. Hinds, E. Hugues, V. Pichanick, Phys. Lett. **78A**, 322 (1980)
8. K.C. Brog, T.G. Eck, H. Wider, Phys. Rev. **153**, 91 (1966)
9. W. Nagourney, W. Happer, Phys. Rev. A **17**, 1394 (1978)
10. G.J. Ritter, Can. J. Phys. **43**, 770 (1965)
11. H. Orth, H. Ackermann, E.W. Otten, Z. Phys. A **273**, 221 (1975)
12. E. Arimondo, M. Inguscio, P. Violino, Rev. Mod. Phys. **49**, 31 (1977)
13. L.J. Radziemski, R. Engleman, J.W. Brault, Phys. Rev. A **52**, 4462 (1995)
14. C.J. Sansonetti, B. Richou, R. Engleman, L.J. Radziemski, Phys. Rev. A **52**, 2682 (1995)
15. R. Mariella, Appl. Phys. Lett. **35**, 580 (1979)
16. M. Fuchs, H.G. Rubahn, Z. Phys. D **2**, 253 (1986)
17. L. Windholz, H. Jager, M. Musso, G. Zerza, Z. Phys. D **16**, 41 (1990)
18. C. Umfer, L. Windholz, M. Musso, Z. Phys. D **25**, 23 (1992)
19. W. Scherf, O. Khait, H. Jager, L. Windholz, Z. Phys. D **36**, 31 (1996)
20. W.A. van Wijngaarden, Adv. At. Mol. Opt. Phys. **36**, 141 (1996); W.A. van Wijngaarden, Proc. Atom. Phys. **16**, 305 (1998)
21. A. Beckmann, K.D. Bokle, D. Elke, Z. Phys. **270**, 173 (1974)
22. J. Carlsson, L. Stuesson, Z. Phys. D **14**, 281 (1989)
23. H.J. Metcalf, P. van der Straten, *Laser Cooling & Trapping* (Springer, 1999)
24. J. Walls, Masters thesis, York University, 2001
25. Z.C. Yan, G.W.F. Drake, Phys. Rev. A **66**, 042504 (2002)